AIAA 82-0361R

Synergetic Maneuvering of Winged Spacecraft for Orbital Plane Change

Hideo Ikawa* and Thomas F. Rudiger†
Rockwell International, Downey, California

The maneuverable re-entry research vehicle is a Shuttle-borne spacecraft designed for hypersonic flight experiments. Its winged configuration permits demonstration of a synergetic maneuver for changing the orientation of a spacecraft's orbital plane. The maneuver consists of 1) retroimpulse and an unpowered descent into the atmosphere; 2) a powered aerodynamic turn; and 3) a reboost and injection into the new orbit. The steering profile must provide the required plane change without violating the vehicle's aerodynamic and aeroheating constraints. The synergetic maneuver, whose effectiveness is Earth-position oriented, provides more plane change for a given vehicle mass and propellant supply than the purely orbital method. The duration of the synergetic maneuver is critical to its efficiency, and high-lift, steep-bank flight is found to produce better performance than flight at maximum lift-drag ratio.

Nomenclature

Az	= heading azimuth, deg
C_L, C_D	= lift and drag coefficients, respectively
D	= drag, N
g	= gravitational constant, 9.8 m/s^2
h	= altitude from Earth surface, km
H	= altitude from Earth center $(Re+h)$, km
i	= inclination angle, deg
I_{sp}	= vacuum specific impulse, s
L/D	= lift-drag ratio
M	= $(L/D)/(L/D)_0$
q_∞	= dynamic pressure, N/m^2
R_e	= mean Earth radius, km
R_g	= turning range $(R_T \times \Delta\theta_T)$, km
R_T	= turning radius, km
S	= vehicle reference area, m^2
T	= thrust, N
Δt	= incremental time, s
U	= argument of latitude, deg
V_{eo}	= Earth rotational velocity at equator, km/s
V_i	= inertial velocity, km/s
V_R	= relative velocity with respect to atmosphere, km/s
W	= vehicle weight, kg
$\dot{W}_F$	= propellant consumption rate, kg/s
α	= angle of attack, deg
λ	= incidental longitude measured from node, deg
$\Delta\theta_T$	= incremental turning angle, deg
ρ	= air density, kg/m^3
ϕ_B	= bank angle, deg
ϕ_L	= latitude, deg

Subscript

AT	= aerodynamic turning

Introduction

THE successful flight of the Space Shuttle has demonstrated the feasibility of controlling the flight of a winged re-entry vehicle to a landing at a prescribed location. This demonstration of aerodynamic control at high altitude and hypersonic speed opens the door to a realistic consideration of other maneuvering capabilities of winged space vehicles. Furthermore, the cargo-carrying capability of the Space Transportation System has paved the way for using winged recoverable spacecraft in orbit. If such a vehicle becomes a reality, the abilities to make synergetic maneuvers and select a landing site may be valuable mission assets.

This paper presents and discusses the results of an analysis of the synergetic plane change maneuver. The analysis was performed as part of the maneuverable re-entry research vehicle (MRRV) project.[1,2] The MRRV (Fig. 1) is a hypersonic vehicle designed to be placed in low-Earth orbit (LEO) by the Space Shuttle and to return to Earth autonomously. The primary purpose of the MRRV is to conduct hypersonic atmospheric flight experiments outside the Space Shuttle flight corridor and to bridge the technology gap between the Shuttle and the ground base tests.[1-3] One of the theories that can be put into practice is the synergetic plane change maneuver (SM). Its winged configuration permits a maneuver which makes use of an aerodynamic turn to alter the orientation of a spacecraft's orbital plane. The maneuver basically consists of 1) retroimpulse followed by an unpowered descent into the atmosphere, 2) a powered turn, and 3) a reboost and injection into a new orbit, Fig. 2. The altitude of the new orbit may be the same as the original or different, but its inclination and node location are different.

The principal objective of this study was to maximize the plane inclination change when SM is performed over a spherical Earth. It also addressed the effective maneuver for maximizing the longitudinal shift of the ascending node. The previous SM studies[4,5] were concentrated on inclination change, which was determined by equating the heading angle change, by neglecting the performance penalties induced by the Earth shape and the aeroheating.

The study demonstrates that the effectiveness of SM is Earth-position oriented and aeroheating constraints prohibit the more maneuverable operations in high dynamic pressure regime. Finding an operational region (altitude-velocity) within the vehicle's aerodynamic performance characteristics and the aeroheating constraints becomes the major factor. Consequently, the net inclination change by SM over the Earth is less than the ideal SM case; however, it offers an advantage over the purely orbital method for the same ΔV expenditure. For example, a plane change of approximately 19 deg has been found possible within the 1667 K (3000°R) temperature limit behind the MRRV nose. By comparison, an all-propulsive plane change in orbit, using the same vehicle, would be limited to about 14.5 deg. To the best of the authors'

Presented as Paper 82-0361 at the AIAA 20th Aerospace Sciences Meeting, Orlando, Fla., Jan. 11-14, 1982; submitted Jan. 22, 1982; revision received June 21, 1982.

*Member of Technical Staff, Space Operations/Integration & Satellite Systems Division. Member AIAA.

†Supervisor, Flight Mechanics and Mission Analysis, Space Operations/Integration & Satellite Systems Division.

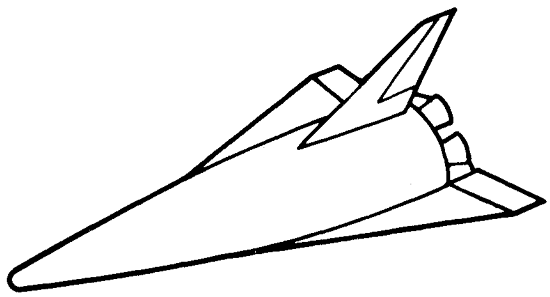

Fig. 1 Maneuverable re-entry research vehicle (MRRV) configuration.

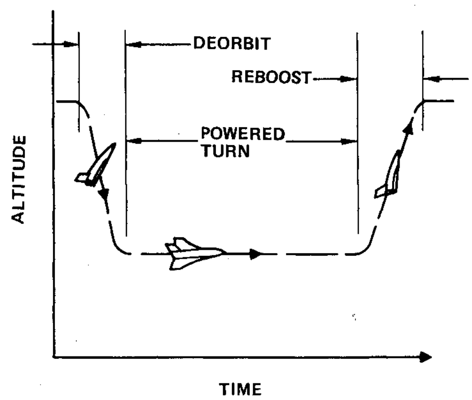

Fig. 2 Synergetic maneuvering trajectory.

knowledge, no previous investigation in this context has been made.

Fuel economy alone may not justify the complexity of the synergetic maneuver, but the maneuver may serve a useful purpose in missions where penetration of the atmosphere is required for other reasons. The maneuver is relatively difficult to track, it ends in an orbit that is difficult to predict rapidly, and it may be performed outside the view of a possible adversary.

Theoretical Development

This paper concentrates on the aerodynamic turning portion of the maneuver. The equations of motion are discussed, assuming a spherical Earth. It also assumes that the vehicle cruises on a great circle plane and that the plane change is performed at constant altitude with constant velocity (such as in a circular orbit). This condition is selected because it simplifies the problem and demonstrates the essentials of SM without loss of generality (WLOG). Also, the aeroheating constraints preclude the large altitude-velocity variations. The vehicle position at any time is defined by a right spherical triangle relationship (Fig. 3) and the following set of equations:

$$\cos i = \cos\phi_L \sin Az \tag{1a}$$

$$\sin i = \sin\phi_L / \sin U \tag{1b}$$

$$\sin\lambda = \tan\phi_L / \tan i \tag{1c}$$

$$\tan\lambda = \cos i \tan U \tag{1d}$$

$$\cos\lambda = \cos Az / \sin i \tag{1e}$$

The rate of change for orbit plane inclination angle is determined by differentiation of Eq. (1a):

$$\frac{di}{dt} = \frac{1}{\sin i}\left\{\sin Az \sin\phi_L \frac{d\phi_L}{dt} - \cos\phi_L \cos Az \frac{dAz}{dt}\right\} \tag{2}$$

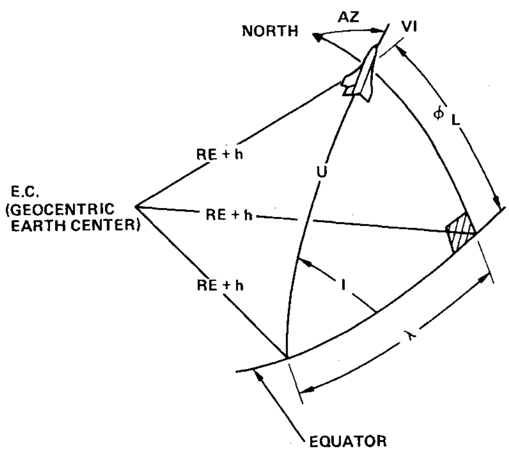

Fig. 3 Right spherical triangle relationship.

On an unperturbed trajectory, $di/dt = 0$; hence, the change in vehicle heading (azimuth) is proportional to the rate of latitude variation

$$\left(\frac{dAz}{dt}\right)_{\Delta i=0} = \tan Az \tan\phi_L \left(\frac{d\phi_L}{dt}\right)_{\Delta i=0} \tag{3}$$

An inclination change (Δi) is produced when the vehicle heading is perturbed from this relationship. The perturbation of vehicle heading is executed by aerodynamic turning during constant-speed powered cruise. Ideally, vehicle inertial velocity is assumed to be constant. For the sake of simplicity WLOG, the aerodynamic turning maneuver is assumed to be performed in a plane normal to the local altitude vector. The turning radius (Fig. 4) is defined as

$$R_g = V_i \Delta t = R_T \Delta\theta_T \tag{4}$$

$$R_T = \frac{V_i \Delta t}{\Delta\theta_T} = \frac{V_i}{(dAz/dt)_{AT}} \tag{5}$$

where the angular rate of turning is equivalent to the change of heading rate produced by aerodynamic turning

$$\left(\frac{dAz}{dt}\right)_{AT} = \lim_{\Delta t \to 0} \frac{\Delta\theta_T}{\Delta t} \tag{6}$$

The equilibrium force balance for turning is

$$F = \frac{WV_i^2}{gR_T} = C_L \frac{\rho V_R^2}{2} S \sin\phi_B \tag{7}$$

and the lift requirement is

$$\frac{W}{S}\left\{1 - \frac{V_i^2}{gH}\right\} = C_L \frac{\rho V_R^2}{2} \cos\phi_B \tag{8a}$$

where ϕ_B is the vehicle bank angle, which can be expressed explicitly as

$$\cos\phi_B = \frac{W}{S}\,\frac{1 - V_i^2/gH}{C_L q_\infty} \tag{8b}$$

where

$$q_\infty = \tfrac{1}{2}\rho V_R^2 \tag{9}$$

Dynamic pressure is defined by the relative velocity with respect to the Earth's atmosphere. The relative velocity (V_R)

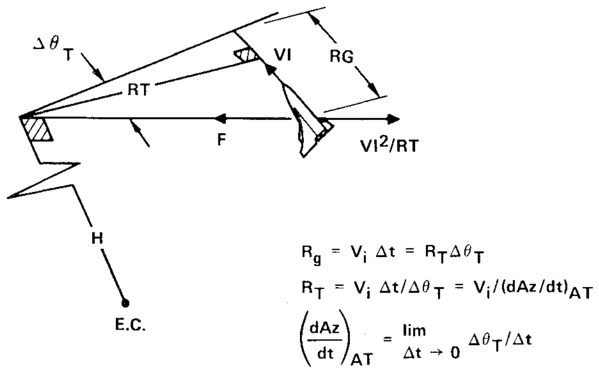

Fig. 4 Geometry for turning maneuver.

varies with vehicle position as defined by latitude and local heading azimuth:

$$V_R^2 = V_i^2\left\{1 - \frac{2V_{eo}}{V_i}\sin Az\cos\phi_L + \left(\frac{V_{eo}}{V_i}\right)^2\cos^2\phi_L\right\} \tag{10}$$

When Eq. (5) is substituted into Eq. (7), the rate of change for the heading azimuth produced by aerodynamic turning can be re-expressed as

$$\left(\frac{\mathrm{d}Az}{\mathrm{d}t}\right)_{\mathrm{AT}} = \frac{gC_L q_\infty \sin\phi_B}{(W/S)\,V_i} \tag{11}$$

The following analysis illustrates the relationship between the rate of heading azimuth change and the rate of propellant consumption. The propellant consumption rate is

$$\dot{W}_F = T/I_{sp} \tag{12}$$

For sake of simplicity WLOG, the thrust vectoring effect with vehicle attitude can be ignored, and the rocket thrust is set equal to the vehicle drag for an unaccelerated powered cruise. The thrust is assumed to be adjustable.

$$T = -D = -C_D q_\infty S \tag{13}$$

The required drag coefficient for balanced flight can be expressed as

$$C_D = \frac{-\dot{W}_F I_{sp}}{q_\infty S} \tag{14}$$

and the lift coefficient can be described by the same parameters

$$C_L = -\frac{(L/D)\,\dot{W}_F I_{sp}}{q_\infty S} \tag{15}$$

If the lift coefficient in Eq. (11) is replaced and the propellant expenditure rate ($\dot{W}_F$) is redefined as a vehicle weight change rate, Eq. (11) can be rewritten as

$$\left(\frac{\mathrm{d}Az}{\mathrm{d}t}\right)_{\mathrm{AT}} = \frac{-gI_{sp}\sin\phi_B}{V_i}\left[\frac{(L/D)}{(W/S)}\,\frac{\mathrm{d}(W/S)}{\mathrm{d}t}\right] \tag{16}$$

The critical parameter is the product of L/D and rate of weight change, as defined in

$$\frac{(L/D)}{(W/S)}\,\frac{\mathrm{d}(W/S)}{\mathrm{d}t} = \frac{-C_D(L/D)q_\infty}{(W/S)I_{sp}} < 0 \tag{17}$$

As will be shown later, maximum L/D flight may not necessarily produce the optimal plane change.

Integration of Eq. (16) gives

$$\frac{W}{S} = \frac{W_0}{S}\exp\left\{-\frac{1}{gI_{sp}}\int_t \frac{V_i}{(L/D)\sin\phi_B}\left(\frac{\mathrm{d}Az}{\mathrm{d}t}\right)_{\mathrm{AT}}\mathrm{d}t\right\} \tag{18}$$

In the vacuum environment of the orbit, the propellant expenditure rate is related to ΔV by

$$\frac{W}{S} = \frac{W_0}{S}e^{-\Delta V/gI_{sp}} \tag{19}$$

Equating Eqs. (18) and (19)

$$\Delta V = \int_t \frac{V_i}{(L/D)\sin\phi_B}\left(\frac{\mathrm{d}Az}{\mathrm{d}t}\right)_{\mathrm{AT}}\mathrm{d}t \tag{20}$$

Therefore, the propellant or energy expenditure, represented by ΔV, is proportionally related to the rate of heading azimuth change produced by aerodynamic turning. It must be noted that L/D and bank angle (ϕ_B) can be modulated as vehicle weight changes. Therefore, Eq. (16) must be integrated numerically.

For a vehicle traveling on an unperturbed trajectory with an inertial velocity (V_i), the instantaneous change in argument of latitude (U) is a function of V_i

$$\frac{\mathrm{d}U}{\mathrm{d}t} = \frac{V_i}{H} \tag{21}$$

Differentiation of Eq. (1b) with i as the constant instantaneously gives

$$\left(\frac{\mathrm{d}\phi_L}{\mathrm{d}t}\right)_{\Delta i=0} = \frac{\cos U\sin i}{\cos\phi_L}\,\frac{\mathrm{d}U}{\mathrm{d}t} = \frac{V_i}{H}\cos Az \tag{22}$$

which is also verified geometrically. The rate of heading azimuth produced by the unperturbed trajectory, Eq. (3), can be re-expressed as

$$\left(\frac{\mathrm{d}Az}{\mathrm{d}t}\right)_{\Delta i=0} = \frac{V_i}{H}\sin Az\tan\phi_L \tag{3a}$$

Therefore, the total heading change is produced by two components given by Eqs. (3a) and (16)

$$\frac{\mathrm{d}Az}{\mathrm{d}t} = \left(\frac{\mathrm{d}Az}{\mathrm{d}t}\right)_{\Delta i=0} + \left(\frac{\mathrm{d}Az}{\mathrm{d}t}\right)_{\mathrm{AT}} \tag{23}$$

Since the inclination can be perturbed by external force only, the rate of inclination change is rewritten as

$$\frac{\mathrm{d}i}{\mathrm{d}t} = -\frac{\cos Az\cos\phi_L}{\sin i}\left(\frac{\mathrm{d}Az}{\mathrm{d}t}\right)_{\mathrm{AT}} \tag{24}$$

The negative sign on the right-hand term implies that increasing inclination angle is induced by reducing the heading azimuth angle when the vehicle is northbound ($0 \le Az \le \pi/2$) and by increasing the heading azimuth angle when the vehicle is southbound ($\pi/2 < Az \le \pi$). Because the direction of heading azimuth is controlled by the $\sin\phi_B$ term, the vehicle must be banked left ($\phi_B < 0$) during northbound flight and right during southbound flight. The bank, therefore, must be reversed at the latitude extremes in order to continue the inclination change in the same direction. Late or premature bank reversal degrades the ability to change inclination.

Orbital plane change generally involves a shift in longitude of the ascending node as well as a change in inclination. Differentiation of Eq. (1d) describes the behavior of the longitudinal change

$$\frac{d\lambda}{dt}=\frac{V_i}{H}\frac{\sin^2 Az}{\cos i}-\frac{\cos Az\tan\phi_L}{\sin i}\frac{di}{dt} \tag{25}$$

where the first term in the right-hand side is produced by vehicle motion on an unperturbed trajectory and the second contribution is induced by the aerodynamic turning maneuver. The new longitude position measured from the original reference point is obtained by integration of Eq. (25)

$$\lambda_j=\lambda_{j-1}+\int_t\frac{d\lambda}{dt}dt \tag{26}$$

With new positional information, i_j, ϕ_{L_j}, λ_j, and Az_j, a new ascending node position with respect to the vehicle position can be determined by

$$\lambda_j'=\sin^{-1}(\tan\phi_{L_j}/\tan i_j) \tag{27}$$

The node shift is defined by

$$(\Delta\lambda_j)_{\text{node}}=\lambda_j-\lambda_j' \tag{28}$$

During the powered cruise, vehicle mass decreases as the propellant is consumed. In order to maintain constant altitude flight as the mass changes, angle of attack and bank angle must be modulated. The required bank modulation is defined by differentiation of Eq. (8b) and can be expressed as

$$\frac{d\phi_B}{dt}=\frac{\cos\phi_B}{\sin\phi_B}\left\{\frac{1}{q_\infty}\frac{dq_\infty}{dt}+\frac{1}{C_L}\frac{dC_L}{dt}-\frac{1}{W/S}\frac{d(W/S)}{dt}\right\} \tag{29}$$

for constant altitude. Bank modulation is influenced by variation in vehicle mass Eq. (17), dynamic pressure Eq. (30), and lift coefficient Eq. (31).

$$\frac{1}{q_\infty}\frac{dq_\infty}{dt}=\frac{2V_iV_{eo}}{V_R^2}\left\{\left(\sin Az-\frac{V_{eo}}{V_i}\cos\phi_L\right)\sin\phi_L\frac{d\phi_L}{dt}-\cos Az\cos\phi_L\frac{dAz}{dt}\right\}\frac{1}{C_L}\frac{dC_L}{dt} \tag{30}$$

$$\frac{dC_L}{dt}=\left\{\frac{1}{C_D}\frac{dC_D}{d\alpha}+\frac{1}{L/D}\frac{d(L/D)}{d\alpha}\right\}\frac{d\alpha}{d(W/S)}\frac{d(W/S)}{dt} \tag{31}$$

where angle of attack can be varied with vehicle mass.

Synergetic Maneuver Behavior Near the Equator Crossing and the Trajectory Apex

The synergetic maneuver exhibits particularly interesting behavior when performed near the apex (maximum and minimum latitude) and the equator. An aerodynamic turn can be achieved effectively at any point on the Earth, but its effectiveness for plane change depends upon where it is performed. The inclination is most sensitive to turns at the equator, and the node location is most sensitive to turns at the apexes of the orbit.

The trajectory apex is approached as $\phi_L\to i$ and heading azimuth approaches the due easterly direction (i.e., $Az\to\pi/2$). Defining $\cos Az=\sin(\pi/2-Az)\simeq\epsilon$, Eq. (24) can be rewritten as

$$\frac{di}{dt}\cong\lim_{\epsilon\to 0}-\epsilon\frac{\cos\phi_L}{\sin i}\left(\frac{dAz}{dt}\right)_{AT}\to 0 \tag{24a}$$

Then the rate of longitude change becomes proportional to V_i/H near the apex

$$\frac{d\lambda}{dt}\cong\frac{V_i}{H}\frac{1}{\cos i} \tag{25a}$$

These relationships imply that the inclination change is minimized and the longitude change of the ascending node is maximized at the apex, Fig. 5.

The behavior of the plane change from an equatorial orbit can be observed when the initial conditions of $i=0$, $\phi_L=0$, and $Az=\pi/2$ are applied to Eqs. (24) and (25). Near the equator with a shallow orbital plane inclination, $Az=\pi/2-i$. Then, $\cos Az=\cos(\pi/2-i)\cong i$. On departure from the equtorial orbit, $i\to 0$. These equations are reduced to

$$\frac{di}{dt}\cong-\left(\frac{dAz}{dt}\right)_{AT} \tag{24b}$$

$$\frac{d\lambda}{dt}\cong\lim_{i\to 0}-i\frac{di}{dt}+\frac{V_i}{H}\to\frac{V_i}{H} \tag{25b}$$

For a nonzero inclination angle, both Eqs. (24) and (25) contain no singularity at the equator crossing. Therefore, di/dt is maximized and $d\lambda/dt$ is unaffected by the aerodynamic maneuver at this point, Fig. 5.

In summary, the synergetic maneuver is analyzed by simultaneous integration of Eqs. (17), (22-25), and (29) and by solving Eqs. (27) and (28). As will be shown in the next section, this theory has captured the main ingredient of the synergetic maneuver well.

Results and Discussion

Qualitative Behavior Analysis

To describe the qualitative behavior of orbital plane changes by aerodynamic maneuvering, the results of numerical integration using the theory of the previous section are discussed. The flight conditions used in this portion of the analysis are as follows: $h=72.96$ km (240,000 ft), $\rho=5.927\times10^{-5}$ kg/m^3 (1.15×10^{-7} slug/ft^3), $V_i=7.84$ km/s (25,800 ft/s), $(W/S)_0=411$ kg/m^2 (84 psf), $(W/S)_f=215$ kg/m^2 (44 psf), and $S=11.61$ m^2 (125 ft^2).

The aerodynamic characteristics of MRRV (Ref. 2) are shown in Fig. 6. The maximum L/D of 2.318 ($C_D=0.063$)

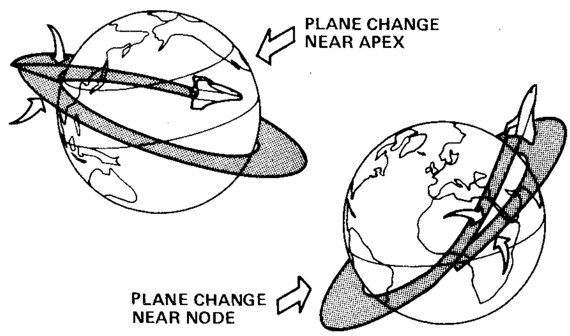

Fig. 5 Schematic view of maximizing inclination change.

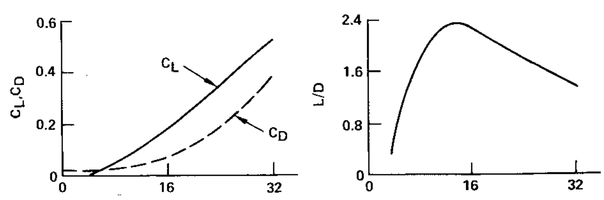

Fig. 6 MRRV hypersonic aerodynamic data ($S_{ref}=11.61$ m^2).

occurs at $\alpha=14$ deg. Angles of attack are prescribed and maintained constant throughout the constant altitude powered cruises. The bank modulation follows the steering law defined by Eq. (29) and is mainly dictated by the mass variation.

A set of inclination angle histories for the aerodynamic maneuver as initiated from the equatorial orbit is shown in Fig. 7. Two distinct regions of optimal inclination change exist for flight between $\alpha=14$ and 30 deg. One region occurs for high angle of attack, where the aerodynamic maneuver is completed before reaching the upper (northernmost) apex. The second region is for a lower angle of attack when the maneuvers terminate on the descending trajectory between the upper and lower apexes. The most ineffective inclination change occurs during $\alpha=18$ deg flight, in which the burnout occurs near the upper apex. The flights for $\alpha=16$ and 24 deg essentially result in identical inclination change but with substantially different durations.

Maximum L/D flight ($\alpha=14$ deg) extends the flight through both upper and lower apexes, thereby reducing the effectiveness for inclination change. This phenomenon can be more readily observed on the overlay plot of inclination and latitude histories, Fig. 8. As the two curves merge at the upper apex, the slope of inclination approaches zero, demonstrating the ineffectiveness of inclination change at the apex. The bank is reversed at this point to continue the inclination change in the same direction. The same phenomenon is observed at the lower apex.

A set of latitude histories for the same flights is shown in B of Fig. 7. The initial slopes of latitude increase proportionately with angle of attack. The variation of the ascending node position with respect to angle of attack is shown in C of Fig. 7. The longitude shift decreases with increasing angles of attack for $\alpha\geq20$ deg, where the turning maneuver is completed on the ascending leg of trajectory. The change in node shows a decreasing trend at higher latitudes on the descending trajectory. It increases again as the vehicle crosses the equator southbound.

These results confirm the argument presented in the previous section; that is, maximum L/D flight does not contribute to optimal inclination change, but does contribute to the shift in position of the ascending node. This statement must be interpreted with caution. It does not imply that a vehicle with inferior L/D design produces better synergetic maneuver performance compared with the high L/D vehicle. The conclusion is that, with a given L/D design, greater inclination change may be achieved with flight attitude of the lower L/D range ($\alpha>\alpha$ at L/D max). For a given C_D, the gain in inclination change capability with improved vehicle design, which produces higher L/D, is shown in Fig. 9 where M is a multiplying factor to improve the vehicle (L/D).

Some interesting observations have been made of the effect of latitude position (for starting the aerodynamic maneuver) on the effectiveness of the inclination change. Maneuvers starting in a 30-deg orbit at initial latitudes of 10, -10, -15, -20, -25, and -30 deg are shown in Fig. 10. In general,

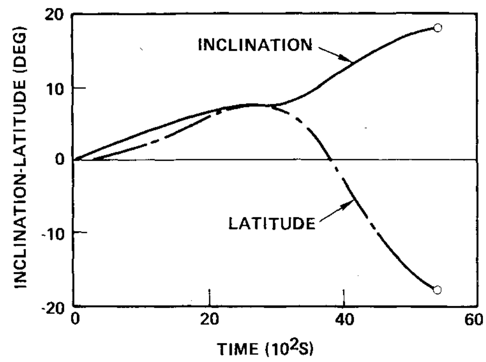

Fig. 8 Inclination-latitude histories; equatorial orbit.

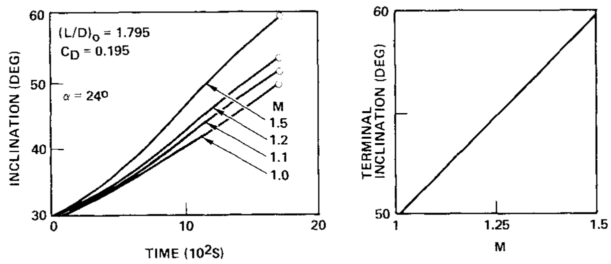

NOTE: $M=(L/D)/(L/D)_0$; $i_0 = 30°$; $\phi_{Lo} = -25°$

Fig. 9 Effect of vehicle (L/D) variation.

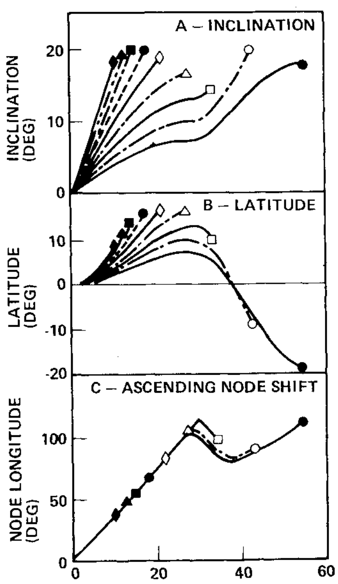

NOTE: ANGLE OF ATTACK VARIATION:
◆30 ▲28 ■26 ●24 ◇22 △20
□18 ○16 ●14

Fig. 7 Synergetic plane change from equatorial orbit ($V_{i0}=7.84$ km/s).

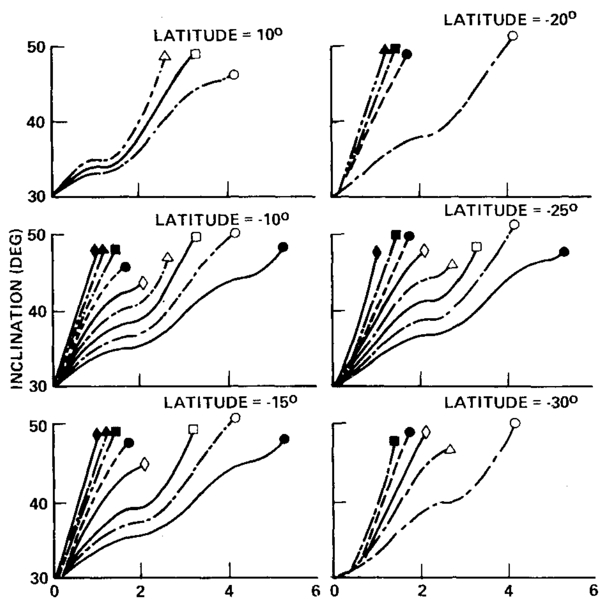

NOTE: $i_0 = 30°$, ϕ_{Lo} VARIATION, $V_{i0} = 7.84$ Km/S
ANGLE OF ATTACK VARIATION: ◆30 ▲28
■26 ●24 ◇22 △20 □18 ○16 ●14

Fig. 10 Synergetic plane change from 30 deg inclined plane.

$\alpha = 16$ deg produced the highest inclination change for all cases investigated, except the one starting from a latitude of 10 deg. In that case, $\alpha = 18$ deg flight was superior. The best latitude to initiate the maneuver is -25 deg, Fig. 11. Longitudinal shift of the ascending node and latitude histories for -25 deg latitude are shown in Fig. 12. The node shifts to the left ($\Delta\lambda < 0$) and to the right ($\Delta\lambda > 0$) of the original position.

In summary, a combination of angle of attack and initial latitude, which allows the vehicle to perform most of the maneuver near the equator, produces the greatest inclination change. To achieve the optimal performance, it is generally advisable to modulate both angle of attack and bank angle in a coordinated manner during the powered cruise.

MRRV Synergetic Maneuver Analysis

In real life, hypersonic flight incurs severe aeroheating effects. The lifting capabilities of the MRRV for a given mass and bank angle are shown in Fig. 13 (altitude vs velocity with α as parameter). The aeroheating constraints are plotted in the same format in Fig. 14. Increased dynamic pressure, which improves aerodynamic performance, is associated with high speed-low altitude flight. However, aeroheating, which is driven proportionally by the total enthalpy flux (ρV_R^3), limits low altitude penetration at high speed. Therefore, a flight corridor for the synergetic maneuver is created by superposition of the curves in Figs. 13 and 14.

The synergetic maneuver analysis for the MRRV was conducted using POST (Program to Optimize Simulated Trajectories).[6] A steering law compatible with the aeroheating constraint was followed. The study results are based on a winged MRRV with dry mass of 2286 kg (5035 lb) and with a useful propellant mass of 2588 kg (5700 lb). There were 2270 kg (5000 lb) of propellant used for the synergetic maneuver, including the reboost into the new orbit. Three throttlable rocket engines of 14,678 N (3300 lb) combined maximum thrust and $I_{sp} = 290$ s were assumed, with control to 1.05 times the drag force to maintain relatively constant cruise velocity.

The heating constraints imposed on the MRRV were 2778 K radiation equilibrium temperature (RET) (5000°R) at the stagnation point on the nose and 1667 K (3000°R) RET on the lower surface. As seen in Fig. 14, the aeroheating constraint is dictated by the temperature limitation on the MRRV station immediately behind the nose (station $x = 0.16$ m).

The trajectory simulation for the synergetic maneuver was initiated at an assumed atmospheric entry altitude of 111.2 km (60 n.mi.) using inertial entry angles between -1.5 and -1.0 deg and inertial entry velocity of 7.86 km/s (25,840 ft/s). A high angle of attack ($\alpha = 40$) was maintained during the descent, and the bank angle was modulated to pull up the vehicle for flare at the altitude suitable for powered cruise. The aeroheating, induced by the relative velocity, forced the aerodynamic turning maneuver into an altitude of 71.628 to 74.676 km (235,000 to 245,000 ft).

As indicated in the previous analysis, high lift and high drag accompanied by steep bank produced greater inclination change than maximum L/D flight. The benefits are threefold. For the required lift balance, the steeply banked vehicle produces a quick turning capability. The high-lift, high-drag configuration shortens cruise time, and the turn can be concentrated nearer to the node. Most important, the shorter cruise time reduces vehicle exposure to the severe aeroheating environment, and the total heat load is minimized.

Data for plane change originating from an equatorial orbit are shown in Fig. 15. The aerodynamic powered cruise period lies between the two solid symbols. The powered cruise is terminated when sufficient propellant remains to attain an inertial (reboost) velocity of 7.9 km/s (26,000 ft/s), which will carry the vehicle above the original 296.5-km (160-n.mi.) orbit. The powered reboost is performed under maximum L/D in the period between the closed and open symbols. The altitude oscillations appearing in B of Fig. 15 are minimized by bank modulation as shown in C of that figure. The altitude oscillation can be eliminated by precisely controlling bank in the POST, through use of the steering law of Eq. (29).

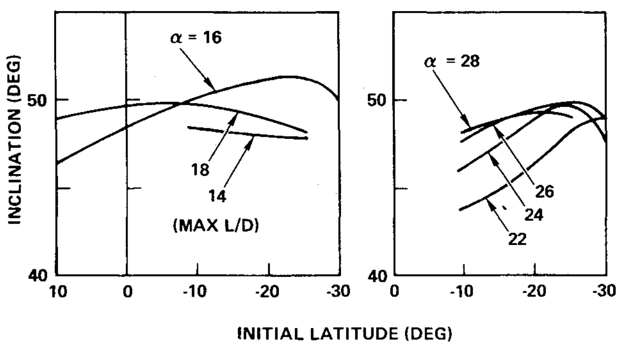

Fig. 11 Inclination angle vs initial latitude ($i_0 = 30$ deg).

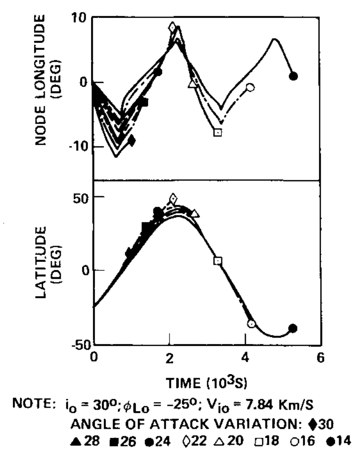

Fig. 12 Ascending node shift and latitude histories.

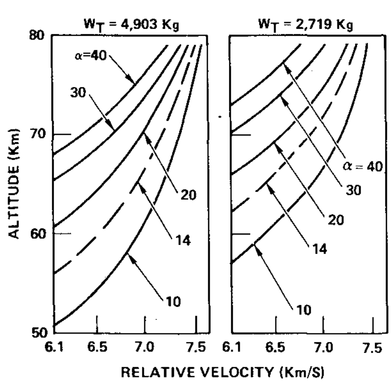

Fig. 13 MRRV lift parameter equatorial orbit ($\phi_B = -30$ deg).

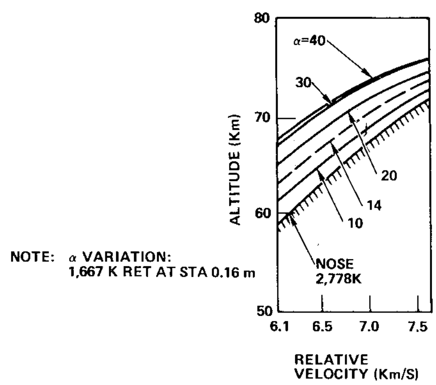

Fig. 14 MRRV aeroheating constraints.

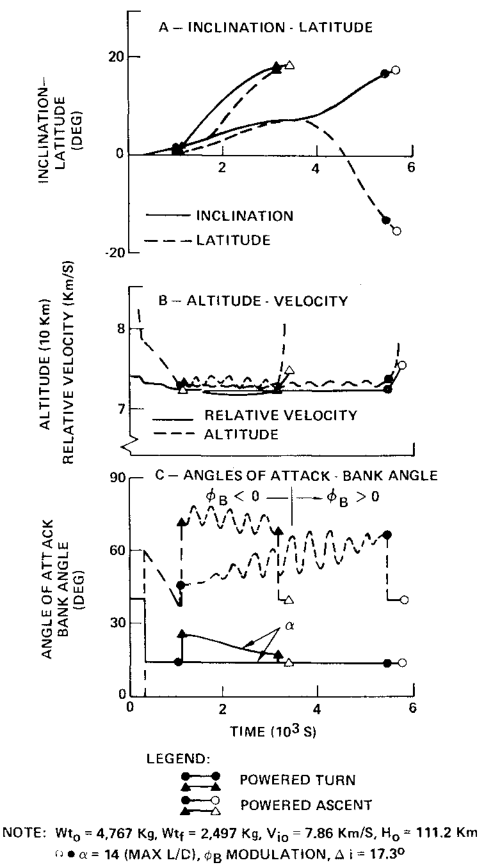

Fig. 15 MRRV synergetic maneuver histories; initial equatorial orbit.

A direct descent trajectory to the powered cruise altitude was achieved by iteration on entry angle. The initial entry conditions from the equatorial orbit were as follows: $h_0 = 111.2$ km (364,560) ft), $\alpha = 40$ deg, $\gamma_{i0} = -1.315$ deg, $\phi_B = -40$ deg, and $V_{i0} = 7.86$ km/s (25,840 ft/s).

The vehicle executed a direct descent and flared ($\gamma_R = 0$) at 72.34 km (237,967 ft) with a relative velocity of 7.224 km/s (23,763 ft/s). The elapsed time was 280 s, considerably shorter than previous attempts. The pertinent data are shown in Fig. 16. Angle of attack was varied from 26 to 19 deg during the powered turning maneuver, and bank angle was modulated about an average of 70 deg. An inclination change of 20.8 deg occurred in 2033 s. The 1667 K radiation equilibrium temperature (3000°R) criterion was exceeded by less than 56 K (100°R). The altitude and thrust oscillations can be minimized by further control of the bank angle, as discussed earlier.

Incremental inclination angle vs vehicle mass (propellant expenditure) is shown in Fig. 17. One hundred and thirty-six kg (300 lb) of propellant are assumed expended during the deorbiting maneuver. Therefore, the initial vehicle mass for executing aerodynamic maneuver is 4767 kg (10,500 lb). The total propellant [2270 kg (5000 lb)] has been allocated for the atmospheric and reboosting maneuvers, from which approximately 1816 kg (4000 lb) are expended for the turning maneuver. An additional 182 kg (400 lb) of propellant remain in the MRRV for future requirements.

Figure 17 shows that the gradient of $di/d(W/S)$ becomes zero as the trajectory apex is approached, attesting to the inefficiency of plane change maneuvers near this point. For a flat Earth with a rectangular grid, the inclination change would be directly proportional to the aerodynamic heading change. In this case, flight with maximum L/D provides the most effective plane change capabilities. However, the synergetic plane change maneuver is performed over a

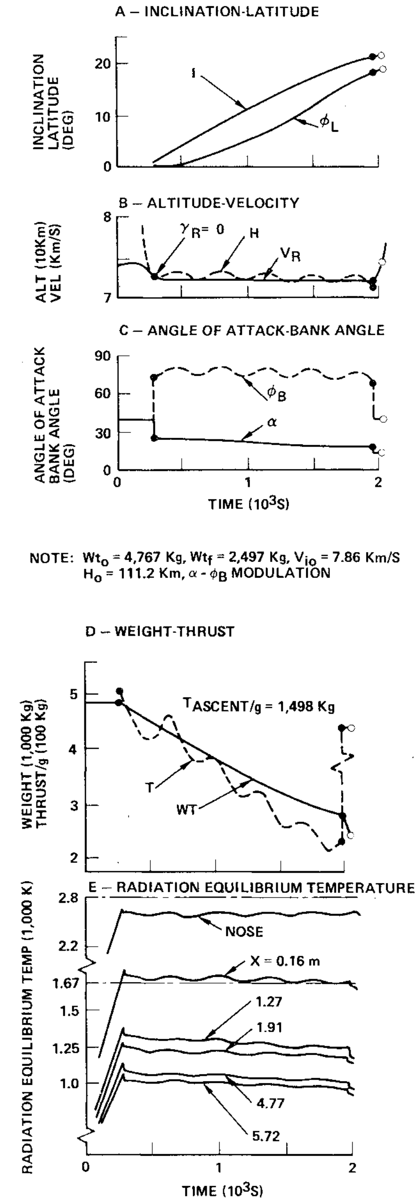

Fig. 16 MRRV synergetic maneuver histories; direct descent from entry point to powered cruise altitude.

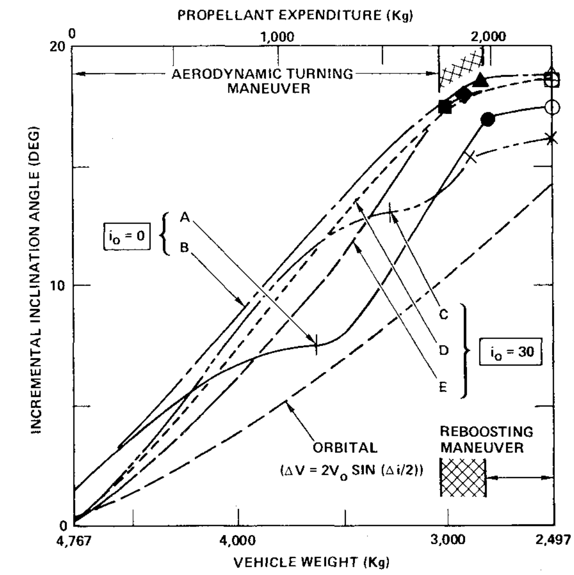

Fig. 17 MRRV incremental inclination angle vs vehicle weight.

spherical Earth, and the extended range characteristic of maximum L/D flight induces a performance loss near the apex. The overall assessment of this study is that greater inclination change is possible with the synergetic maneuver than with the purely orbital method using impulsive forces.

Conclusion

The feasibility of changing orbital plane by synergetic maneuvering of a high L/D winged vehicle is established. The simple theory, verified by POST, shows that the effectiveness of SM is Earth-position oriented and high lift-high drag flight is superior to maximum L/D flight, especially with the presence of aeroheating constraints. Additional performance improvements may be realized by optimization technique, which derivation will be left for the future undertaking. Aerodynamic maneuvers can be enhanced at flight in high dynamic pressure regime; however, aeroheating constraints prohibit the lower altitude penetration with high velocity and large altitude-velocity variations.

Acknowledgments

The methodology and results described in this paper were developed in part for the Air Force Wright Aeronautical Laboratories under Contract F33615-80-C-3015, Concept Evaluation of a Maneuverable Re-Entry Research Vehicle (MRRV) and Related Experiments. The authors express their appreciation to Paul Lane Jr. and Rick Norris of AFWAL/FIMS for their cooperation.

References

[1]Hoge, H.J., "Concept Evaluation of a Maneuverable Re-Entry Research Vehicle (MRRV) and Related Experiments," AFWAL-TR-81-3125, AFWAL/FIMS Contract F33615-80-C-3015, Nov. 1981.

[2]Hoge, H.J., "Development of Military Hypersonic Flight Test Experiments," AFFDL-TR-79-3159, AFFDL/FXS Contract F33615-78-C-3020, Nov. 1979.

[3]Draper, A.C., Lane P., Jr. and Zima, W.P., "A Flight Research Vehicle To Bridge Shuttle and Hypersonic Aircraft Technology," AIAA Paper 77-1165, 1977.

[4]Paine, J.P., "Use of Lifting Reentry Vehicles for Synergetic Maneuvers," *Journal of Spacecraft and Rockets,* Vol. 4, May 1967, pp. 698-700.

[5]Wallner, E.P. and Camiel, J.J., "Plane Change Split in Circular Orbit," *Journal of Spacecraft and Rockets,* Vol. 3, April 1966, pp. 603-605.

[6]Bauer, G.L., Cornick, D.E., Habeger, A.R., Peterson, F.M., and Stevenson, R., "Program to Optimize Simulated Trajectories (POST)," Vol. II, Utilization Manual, NASA CR-132690, April 1975.